Rotational Stiffness of Rectangular Hollow Sections Composite Joints

L. A. P. Silva[1]; L. F. N. Neves[2]; and F. C. T. Gomes[3]

Abstract: Joints in steel rectangular hollow sections filled with concrete present the added difficulty of involving the deformability of the connected faces in bending. This implies that, unless a good estimate of the moment-rotation curve can be obtained, complex and expensive detailing is required to ensure a fairly rigid response of the joint. A first step to achieve the objective of predicting the behavior of such a joint corresponds to an assessment of the initial stiffness of the joint. Starting with a brief review of the current state-of-the-art in the behavior of joints in hollow sections, this paper presents and discusses an analytical model based on an equivalent strip of the loaded face. A simple solution based on this model that has been calibrated with numerical simulations is also derived. The main parameters considered are the thickness of the loaded face and the dimensions of the loading area. Comparisons with some available numerical and experimental results are quite encouraging.

DOI: 10.1061/(ASCE)0733-9445(2003)129:4(487)

CE Database subject headings: Steel structures; Joints; Composite materials; Hollow sections; Stiffness.

Introduction

Composite structures combine the advantages of steel and concrete. In particular, composite columns have high ductility with stiffness and strength enhanced by the presence of concrete. There are two types of composite columns: steel sections encased in concrete and concrete-filled steel hollow sections (circular and rectangular). Comparing the latter system with steel hollow sections alone, it presents the added advantage of enhancing fire resistance and strength, while comparing to a standard reinforced concrete column it improves resistance and ductility through minimization of steel rebars and continuous confinement of concrete and also productivity through elimination of the formwork.

Using concrete-filled hollow sections in composite columns requires proper knowledge of the behavior of the joint between I-beams and rectangular hollow sections (RHS), being one of the common solutions employed in composite construction, as shown in Fig. 1.

Recent research developments in steel and composite joints (Weynand et al. 1995) over the traditional approach of pinned or fully rigid response allow the prediction of the real moment-rotation ($M-\phi$) behavior of joints. The ''component method,'' currently widely accepted by the scientific community and adopted by some code regulations (Eurocode 3 1992), consists of a simplified mechanical model composed of extensional springs and rigid links, whereby the connection is simulated by an appropriate choice of rigid and flexible components. These components represent a specific part of a connection that, dependent on the type of loading, makes an identified contribution to one or more of its structural properties. A typical component model for a RHS composite joint is illustrated in Fig. 2, the relevant components being (K_5/K_6) end-plate or flange cleat in bending, (K_7) beam flange and web in compression, (K_8) beam web in tension, (K_{10}) bolts in tension, (K_{11}) bolts in shear, (K_{13}) welds, and (K_{14}) column web/loaded chord in bending. In general, each of these components is characterized by a nonlinear force-deformation curve, although simpler idealizations are possible, whenever only the resistance or the initial stiffness of the connection is required. Application of the component method to steel connections requires the following steps:

1. Selection of the relevant (active) components from a global list of components (13 different components currently codified, for example, in Annex J of EC3);
2. Evaluation of the force-deformation response of each component; and
3. Assembly of the active components for the evaluation of the moment-rotation response of the connection, using a representative mechanical model.

Joints between I-beams and rectangular hollow sections present a distinct behavior that differentiates them from major axis joints between I-sections. In fact, the absence of a central stiffening web means that the loaded chord of the column must resist the tensile and compressive forces arising from the beam flanges in bending, akin to a plate supported on its vertical sides. This typical behavior may in fact also be found in weak-axis joints (Neves 1996).

The behavior of joints between concrete-filled rectangular hollow sections and I-beams has been studied by several authors: Matsui (1986); Lu et al. (1993); Vandegans (1996); and Lu and Wardenier (1998). Vandegans (1996) showed that the deformability of the column is due almost exclusively to the deformability of the loaded chord face, that may thus be considered as a clamped plate at the junction with the chord side walls. Reference should

[1]Associate Professor, Civil Engineering Dept., Univ. of Coimbra, Polo II, Pinhal de Marrocos, 3030 Coimbra, Portugal. E-mail: luis_ silva@gipac.pt

[2]Assistant, Civil Engineering Dept., Univ. of Coimbra, Polo II, Pinhal de Marrocos, 3030 Coimbra, Portugal. E-mail: luis@dec.uc.pt

[3]Assistant, Civil Engineering Dept., Univ. of Coimbra, Polo II, Pinhal de Marrocos, 3030 Coimbra, Portugal.

Note. Associate Editor: Mark D. Bowman. Discussion open until September 1, 2003. Separate discussions must be submitted for individual papers. To extend the closing date by one month, a written request must be filed with the ASCE Managing Editor. The manuscript for this paper was submitted for review and possible publication on April 29, 1999; approved on July 15, 2002. This paper is part of the ***Journal of Structural Engineering***, Vol. 129, No. 4, April 1, 2003. ©ASCE, ISSN 0733-9445/2003/4-487–494/$18.00.

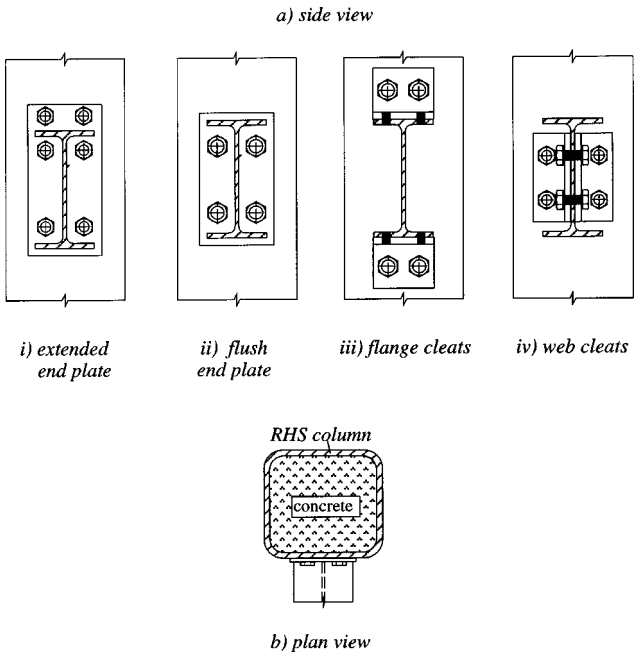

Fig. 1. Typical joint between I-beam and concrete-filled rectangular hollow section

be made to other studies that have been performed on joints between beams and concrete-filled columns that are concerned with circular hollow sections (Shakir-Khalil et al. 1992; Morino et al. 1993; Ricles et al. 1997).

Application of the component method to RHS joints is still not possible given that, according to the philosophy of the method, full characterization of the most relevant component is still unavailable: the chord face loaded in bending and shear, denoted as (K_{14}) in Fig. 2.

Characterization of the behavior of the joint between a RHS and an I-beam requires the identification of its strength, stiffness, and ductility. As far as the strength of the chord face is concerned, the solutions proposed (Gomes et al. 1994; Gomes 1996), in the context of weak-axis joints for single bolt rows in tension, and the adaptation of these models to RHS joints (Vandegans 1995) provide some guidance to the evaluation of strength of RHS joints.

In terms of stiffness, an analytical model for concrete-filled RHS composite joints is proposed which was also developed in the context of weak-axis joints (Neves and Gomes 1996) and is described in detail later in this paper. Finally, besides some observation of experimental evidence of some ductility, fairly limited guidance exists in this area.

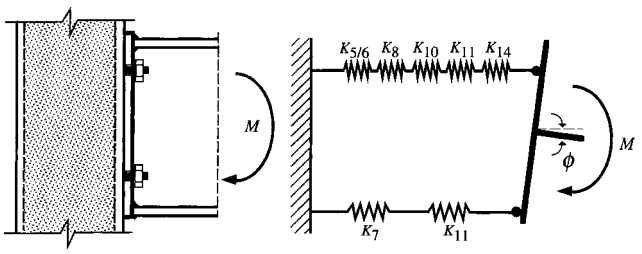

Fig. 2. Component method: Example of spring model for RHS composite joints

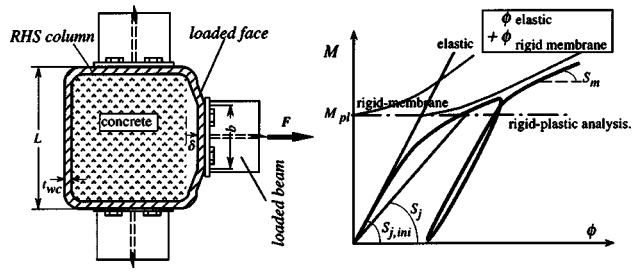

Fig. 3. Geometric characteristics and typical behavior of loaded face in RHS/I-beam joint

Behavior of RHS/I-Beam Joints

Characterization of Moment-Rotation Response

Fig. 3 illustrates the typical rotational behavior of the loaded chord face: M=the moment transmitted to the column, and ϕ=the rotation of the joint resulting from the deformation of the loaded column face. This moment-rotation ($M-\phi$) curve may, in the initial elastic range, be characterized by the initial stiffness $S_{j,\mathrm{ini}}$. Because of the large out-of-plan deformations δ of the loaded chord for higher values of bending moment, often greater than the chord thickness t_{wc}, the typical postlimit stiffening behavior is observed, characteristic of the von Kármán large displacement equations. It is worth noting that neglecting the overstrength of the loaded chord may result in unforeseen overstressing of other joint components (bolts or welds, for example), which may fail suddenly because of their brittle behavior (Neves 1996; Silva et al. 2000).

The load transfer from the beam to the column by the connecting elements shown, as an example, as flange cleats in Fig. 4 could, in the general case, lead to a mechanism involving the upper cleat (tension zone) and the bottom cleat (compression zone). If the distance h in Fig. 4 between these two zones is sufficiently large, these mechanisms will not interact.

For shallow beams where h is short, there is in fact an interaction between areas loaded in tension and compression. In consequence, in these minor-axis or I-beam to a RHS column without concrete filling joints, the yielding mechanism involves the two areas as shown in Gomes (1996). The analytical solution available from these studies for the plastic forces in the upper and lower

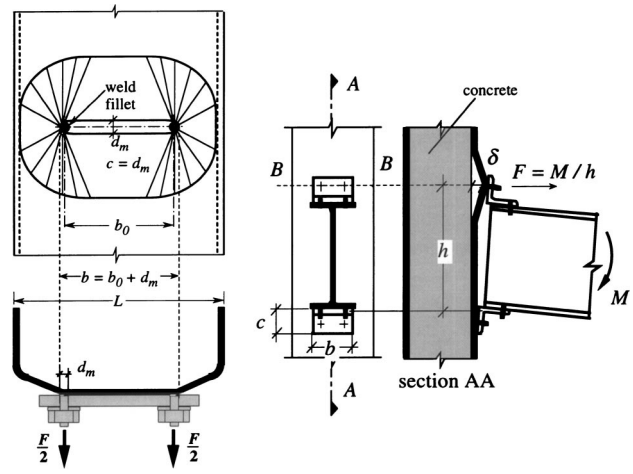

Fig. 4. Yielding mechanism

Table 1. Nonlinear Numerical Simulations for Local Mechanism

Type of analysis	μ	α	β = 0.08	β = 0.25	β = 0.50	β = 0.75
First order elastic-plastic analysis	50	0.05	B000	B250	B500	B750
		0.1	B001	B251	B501	B751
		0.2	B002	B252	B502	B752
	10	0.05	F000	F250	F500	F750
		0.1	F001	F251	F501	F751
		0.2	F002	F252	F502	F752
Second order elastic-plastic analysis	50	0.05	C000	C250	C500	G750
		0.1	C001	C251	C501	G751
		0.2	C002	C252	C502	G752
	10	0.05	G000	G250	G500	G750
		0.1	G001	G251	G501	G751
		0.2	G002	G252	G502	G752

areas shows that there is in fact a drop of resistance. Further studies (Neves 1996) focusing on the stiffness have shown that there is not a drop of stiffness for the tension nor for the compression areas. The drop in plastic moment and rotational stiffness observed in this case results mainly in the reduction of the lever arm, *h*. In practice, joints where such interaction is possible are classified as pinned. Further details on this topic may be found in Gomes (1996) where the boundaries for the type of behavior observed are clearly established.

In the present situation of concrete-filled columns, the infilling concrete supports the compression zone, leading to the out-of-plan deformation of the column face shown in Fig. 4. The yielding mechanism involves the tension zone alone, and the deformation of the compression zone may be neglected (Vandegans 1995), and will not be considered in this paper.

Identification of Relevant Parameters

The development of an analytical model to predict the behavior of a RHS joint requires proper identification of the relevant parameters affecting the behavior of the loaded chord face.

Referring to Figs. 3 and 4, the following two parameters significantly influence the joint behavior:

1. Dimension of loaded area $b \times c$, where b and c are the width and the height of the connecting element.

Here they correspond to the nondimensional parameters $\beta = b/L$ and $\alpha = c/L$ and it is noted that both resistance and stiffness increase with larger loaded areas.

2. Slenderness of the loaded face: $\mu = L/t_{wc}$, where L and t_{wc} are the width and wall thickness of the RHS, respectively.

This parameter plays a major role in the elastic and postplastic stiffness of this joint component. For smaller values of $\mu \approx 10-15$, shear effects become important, reducing the initial stiffness and resulting in possible failure by punching shear. The postlimit stiffness is small because out-of-plan deformations usually remain within small displacement theories (Neves 1996). For large values of μ (>40) shear effects are negligible and postlimit stiffness is quite large, making it difficult to clearly identify what is usually defined as the plastic moment of the joints. Finally, for intermediate values of μ ($15 < \mu < 40$), it is important to account for shear, bending, and membrane effects.

Table 2. Linear Numerical Simulations for Local Mechanism

Type of analysis	μ	α	β = 0.08	β = 0.25	β = 0.50	β = 0.75
First order elastic	30	0.05	L000	L250	L500	L750
		0.1	L001	L251	L501	L751
		0.2	L002	L252	L502	L752
	20	0.05	M000	M250	M500	M750
		0.1	M001	M251	M501	M751
		0.2	M002	M252	M502	F752

Numerical Study

Introduction

To understand the behavior of these joints, and to propose a model to evaluate their initial, secant, and membrane stiffnesses, a parametric study involving all the parameters described above was undertaken (Neves 1996), covering the following ranges for the various parameters: $0.08 \leq \beta \leq 0.75$, $0.05 \leq \alpha \leq 0.2$, $10 \leq \mu \leq 50$. Table 1 shows the full nonlinear numerical simulations performed and the respective parameters. Table 2 shows additional numerical simulations used to obtain further information concerning initial stiffness, where elastic linear analysis was used.

Finite Element Model

The finite element model adopted for the column web is represented in Fig. 5 for the relevant mechanism of the chord face, involving exclusively the tension area. The symmetry of the joint is accounted for, thus requiring only the modeling of one-quarter of the column. Boundary conditions are: Fixed right edge at the connection with the side walls, that is a valid assumption for in-filled concrete RHS sections (Vandegans 1995), lower free edge at a distance equal to L from the symmetry line B, and the adequate support conditions for symmetry lines A and B in Fig. 5 (fixed m_y and F_x for line A and fixed m_x and F_y for line B).

Thick shell elements were used to model the column web because they could cope with the relevant deformations: bending, shear, and membrane. It is noted that for high slenderness of the web (large μ), shear effects are negligible and thin shell elements perform well, whereas for small values of slenderness ($\mu < 15$), second order membrane effects are negligible, and thick plate elements give accurate results.

The finite element mesh has eight-noded thick shell elements in the zone of the plastic mechanism, and four-noded elements in zones that do not affect the shape of the plastic mechanism, where the mesh may be less refined, as seen in Fig. 5. Transition between these zones of different mesh densities should take place away from the loaded area (in the y direction) at least one-half of the length of the column web in the x direction and may be achieved using three-noded triangular shell elements.

In the modeled area, successive mesh refinements led to the adoption of 12 elements to model the half of the loaded face in the x direction, Fig. 5, resulting in a mesh of 186 elements and 540 nodes with 3,240 degrees of freedom. Comparison of the plastic load (obtained from a first order plastic analysis for different mesh densities) to the theoretical plastic load derived in Gomes (1996) confirms this option.

The material model was based on von Mises yield criterion. Strain hardening may be neglected, as it does not affect considerably the $F-\delta$ curve. Fig. 6 shows the effect on the $F-\delta$ curve of the strain hardening for a slenderness of (i) $\mu = 50$ and (ii) $\mu = 10$ (here the applied force F is nondimensionalized with respect to the plastic load F_{pl}, and the column face displacement δ with respect to L, defined in Figs. 3 and 4. The corresponding

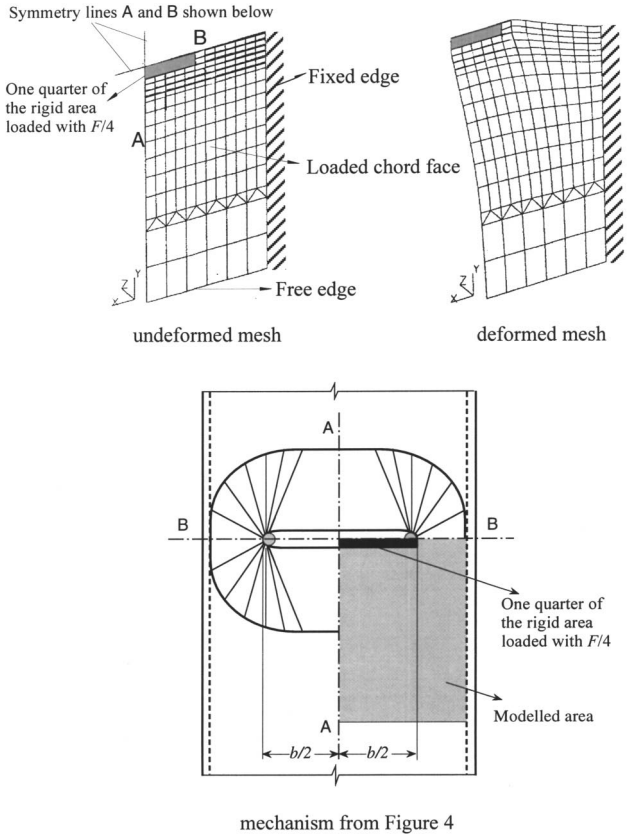

Fig. 5. Finite element meshes for local mechanism in chord face

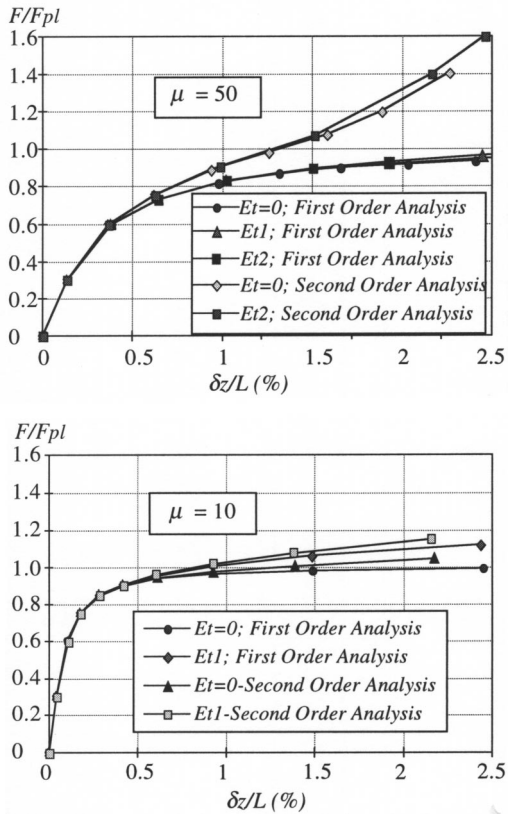

Fig. 6. Effect of strain hardening

hardening moduli were $E_t=0$, $E_{t1}=0.003E$, and $E_{t2}=0.02E$. It is interesting to observe that for a high slenderness, curves with and without strain hardening are hard to distinguish. The same qualitative results have been published (Korol and Mirza 1982) for comparable situations of RHS joints.

Load was applied in four nodes of the modeled area, representing one-quarter of the total load due to the symmetry. The starting load was 30% of the theoretical plastic load, for which no yielding was observed. After this level, incrementation of load was automatic with a maximum step load limited to 30% of the theoretical plastic load. It was based on the Newton–Raphson algorithm until the actual stiffness of the structure reaches 50% of the initial stiffness. From this point and until the end of the process (control of the displacement under the loaded area) incrementation was based in the arc length method. In each load increment convergence was associated to the following criteria that were adopted after calibration: (i) Norm of the residual forces less than 0.1% of the norm of the external forces; (ii) Norm of the iterative displacements less than 0.1% of the norm of the total displacements; and (iii) Work done by the residual forces on the current iteration less than 0.1% of the work done by the external forces on the first iteration.

Calibration of Finite Element Model

Three types of analysis have been performed (Neves 1996): elastic, elastic-plastic, and second order elastic-plastic (material and geometric nonlinearities), using the finite element package LUSAS (1996). Validation of the described numerical model was based upon comparison with three sets of results.

Qualitative comparison with other numerical models. For minor-axis joints (Jaspart et al. 1995), for joints between hot rolled sections and RHS (Ting et al. 1991), and for RHS filled with concrete (Vandegans 1996), numerical models with similar characteristics to the model developed by the authors are described. In particular, the mesh geometry, the adoption of thick shell elements, and neglecting the strain hardening effect are common aspects. In some of the studies, thin shell elements were used, but the slenderness of the plates justified so. The better results achieved with eight-noded elements, compared to four-noded elements have also been referred. From the above studies, qualitative conclusions in close agreement with the present work could be drawn: behavior for large displacements, influence of the size of the loaded area, and slenderness, among others.

Comparison of the numerical values for F_{pl} with the corresponding theoretical values. All the plastic force values F_{pl}, obtained from first order finite element analysis, were compared with the corresponding theoretical values established in Gomes et al. (1994) and Gomes (1996). Excellent correspondence was observed (Neves 1996), with a maximum error for the whole range of parameters studied, μ, β, and α of $\pm 5\%$.

Comparison with experimental results. A considerable number of minor-axis joints laboratory tests (where as already pointed out the column web has a similar behavior to the loaded chord face) have been performed at the University of Liège (Gomes et al. 1994; Jaspart et al. 1995). These included bolted and directly welded beams to the column web. In these tests, setup allowed the measurement of the deformation of the column web alone, thus enabling direct comparison with the numerical models, as well as the present proposals for the stiffness evaluation, and the proposals for the plastic force or moment (Gomes 1996). Good agreement was found when comparing $M-\phi$ numerical and experimental curves, thus validating the numerical model. Fig. 7 shows the comparison of this numerical model with two of the above

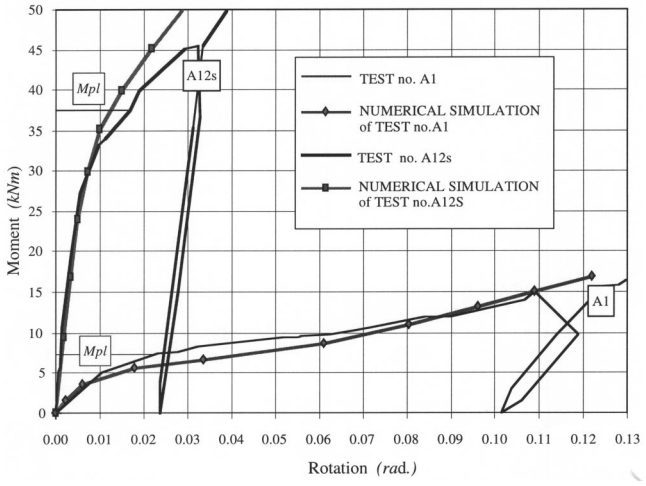

Fig. 7. Comparison of two test curves from Gomes (1996) with corresponding curves obtained from numerical simulations performed by the writers

referred tests. Further details of this model may be found in Neves (1996) and Neves and Gomes (1999).

Analytical Model for Component Column Web in Bending (K_{14})

Initial Stiffness, $S_{j,\text{ini}}$

The initial (or elastic) stiffness is the initial slope of the $M-\phi$ (or $F-\delta$) curve, Fig. 3. The model derived in Neves (1996) for the calculation of the initial stiffness is shown in Fig. 8 and consists of a plate supported at the intersection with the side chord walls (Vandegans 1995) and free in the other borders. This plate has a length L (Figs. 3 and 8) and a width l_{eff} calculated from

$$l_{\text{eff}}=c+(L-b)\tan\theta \tag{1}$$

$$\frac{l_{\text{eff}}}{L}=\alpha+(1-\beta)\tan\theta \tag{2}$$

The theoretical initial (extensional) stiffness of this strip, computing both flexural and shear deformations, may be easily expressed by

$$S_i=\frac{2El_{\text{eff}}t_{wc}^3}{a^3+2(1+\upsilon)at_{wc}^2} \tag{3}$$

where

$$a=\frac{1}{2}(L-b) \tag{4}$$

Introducing Eqs. (2) and (4) in Eq. (3), taking Poisson's ratio $\nu=0.3$, and introducing the two coefficients k_1 and k_2, the following expression is obtained:

$$S_i=\frac{Et_{wc}^3}{L^2}16\frac{\alpha+(1-\beta)\tan\theta}{(1-\beta)^3+10.4(k_1-k_2\beta)/\mu^2} \tag{5}$$

The term

$$\frac{10.4(k_1-k_2\beta)}{\mu^2}$$

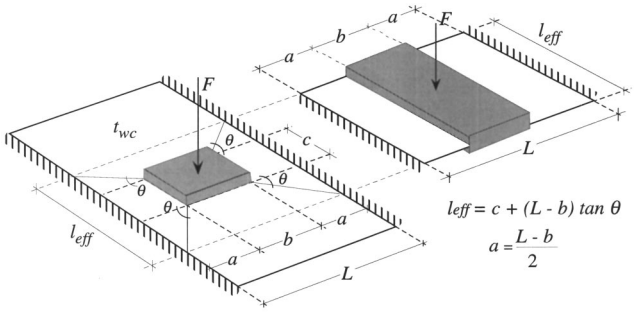

Fig. 8. Chord face loaded by rigid area $b\times c$, and equivalent strip of width l_{eff}

represents the contribution of shear effects to the initial stiffness that play an important role for thick webs as shown in Korol and Mirza (1982). Coefficients k_1 and k_2 allow the adjustment of results from the analytical model to the parametric numerical study described above, and were found to yield good agreement for $k_1=1.5$ and $k_2=1.63$. Angle θ, which controls the strip width, was established by matching the nondimensional initial stiffness obtained from the strip model (Fig. 8),

$$S_{i,a\ \text{dim}}=\frac{S_i}{Et_{wc}^3/L^2} \tag{6}$$

to the empirical nondimensional initial stiffness obtained from the finite element analysis $S_{i,a\ \text{dim}}^{sim}$, and is given by

$$\theta=\tan^{-1}\left[\frac{S_{i,a\ \text{dim}}^{sim}}{16}\left((1-\beta)^2+\frac{10.4}{\mu^2}\frac{(k_1+k_2\beta)}{(1-\beta)}\right)-\frac{\alpha}{1-\beta}\right] \tag{7}$$

Again, calibration within the defined range of the parametric study led to the following approximation for θ as a linear function of β alone:

$$\theta=35-10\beta \tag{8}$$

Some Considerations on Postlimit Behavior

Theoretical results to predict second order behavior of strips and circular plates (Massonet and Save 1972) indicate a parabolic curve followed by a linear function. This postlimit stiffness increases with span-to-thickness ratio (where second order effects are more important). However, if these force-displacement ($F-\delta$) curves are nondimensionalized with respect to the plastic force and to the plate's thickness ($F/F_{\text{pl}}-\delta/t$), the linear part of the postlimit stiffness becomes approximately constant. These conclusions were found to be valid for the numerical simulations described above for the column loaded face, and the displacement corresponding to the transition between the parabolic curve and the straight line approximately corresponds to the thickness of the loaded face. It is thus possible to propose a bilinear model for the postlimit stiffness of the loaded column face (Neves 1996), illustrated in Fig. 9, the two straight lines being given by

$$\frac{F}{F_{\text{pl}}}=\begin{cases}0.9+(f_1+f_2-0.9)\left(\dfrac{\delta}{t}\right) & \text{if } \dfrac{\delta}{t}\leqslant 1 \quad \text{and} \quad \dfrac{F}{F_{\text{pl}}}\geqslant 1\\[2ex] f_1+f_2\left(\dfrac{\delta}{t}\right) & \text{if } \dfrac{\delta}{t}\geqslant 1 \quad \text{and} \quad \dfrac{F}{F_{\text{pl}}}\geqslant 1\end{cases} \tag{9}$$

f_1 corresponding to the intersection with the F/F_{pl} axis of the straight part of the $F/F_{\text{pl}}-\delta/t$ curve and f_2 being the nondimensional membrane stiffness $S_{m,a\ \text{dim}}$, given by

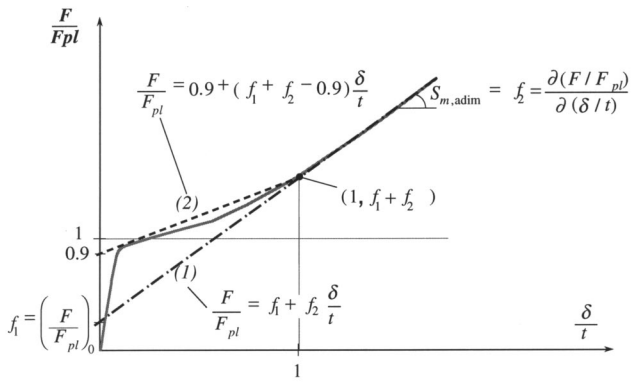

Fig. 9. Bilinear approximation of loaded face postlimit behavior

$$f_1 = -0.24\beta - 0.012\mu + 0.72 \tag{10}$$

$$f_2 = 0.55 + 1.07\alpha + 0.85 \tag{11}$$

these values having been established using a curve-fitting exercise from the results of the parametric study, leading to a safe estimate of the postlimit response of the loaded face.

Comparison with Numerical Results

The proposal for the initial extensional stiffness of the loaded column face [Eq. (5)] is compared in Figs. 10(a–c) with the results from the numerical simulations, for some of the $\mu = L/t_{wc}$ values considered.

In each case, initial stiffness is nondimensionalized with respect to Et_{wc}^3/L^2, and different curves correspond to different values of α. A good agreement could be found comparing results obtained from the application of Eqs. (5)–(8) to those obtained from numerical simulations, with a maximum error in the range of parameters studied of 3% and 9%, respectively, on the unsafe and on the safe side (Neves 1996).

Also shown in Fig. 10 is a previous proposal (Czechowski et al. 1987) for the elastic stiffness of a RHS joint, in a similar situation. Czechowski et al.'s model largely overestimates elastic stiffness, especially for small values of slenderness, μ (Neves 1996).

Vandegans (1996) describes the numerical calculation of the initial stiffness for a flush end plate joint using the finite element program FINELG (1990). The loaded face of the in-filled concrete RHS is modeled as a clamped plate. This finite element model was previously validated by comparisons with tests. The relevant parameters are $\mu = 33.5$, $\beta = 0.49$, and $\alpha = 0.09$. The initial stiffness calculated by Vandegans is 55.7×10^6 N/m (or nondimensionally 49.9), and the application of the proposed model gives 49.5×10^6 N/m (or nondimensionally 44.3).

Application to RHS Composite Joints

In order to illustrate the application of the present model to RHS composite joints, two alternative configurations were selected: (1) flange cleat and (2) extended end-plate. The geometry for these examples was taken from Vandegans (1995), together with the corresponding experimental test results and is illustrated in Fig. 11.

From the component model of Fig. 2, the rotational stiffness of the joint, $S_{j,\mathrm{ini}}$, follows from

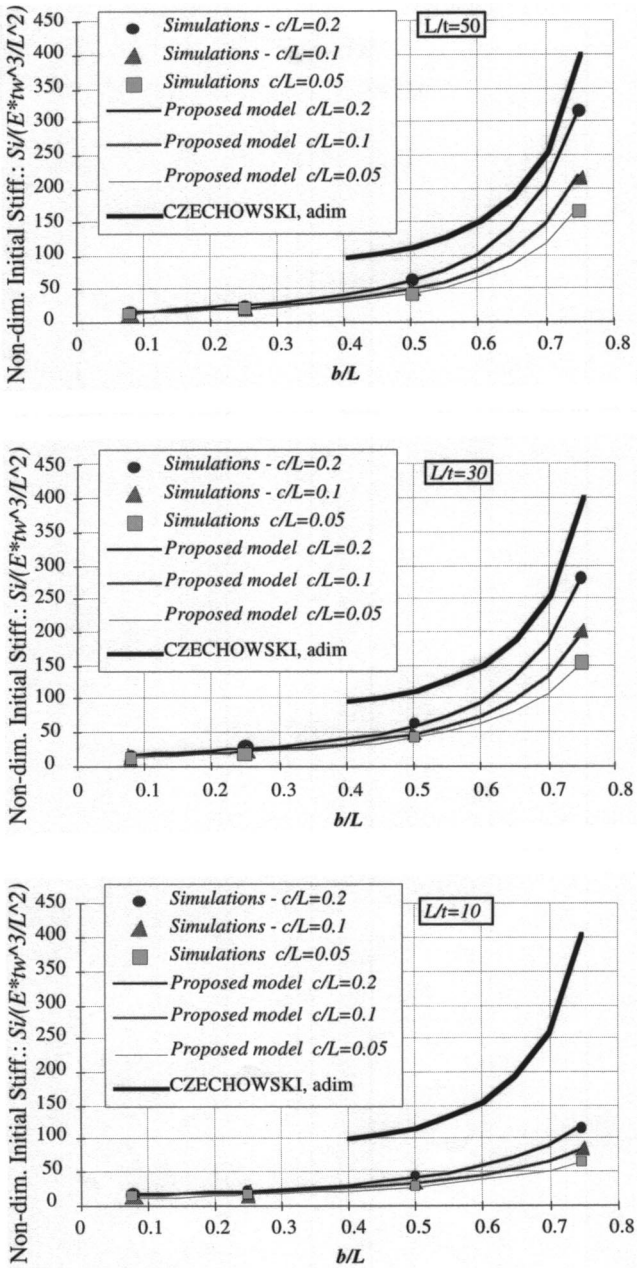

Fig. 10. Variation of initial extensional stiffness with geometrical parameters. Comparison between proposal model, numerical simulations, and Czechowski et al.'s model.

$$S_{j,\mathrm{ini}} = \frac{M}{\phi} = \frac{h^2}{\sum (1/EK_i) + 1/S_{i1} + 1/S_{i2}} \approx \frac{h^2}{\sum (1/EK_i) + 1/S_{i1}} \tag{12}$$

where E = the Young modulus; K_i = the relevant stiffness coefficients given in Annex J of Eurocode 3 for components K_1, K_2, and K_{10}; and S_{i1} and S_{i2} are obtained from Eqs. (5) and (8). It is noted that, in the present situation of concrete-filled columns, where the in-filling concrete supports the compression zone, the term $1/S_{i2}$ is negligible, as shown in Vandegans (1995). According to the Eurocode notation, the stiffness component K_{14} is

$$K_{14} = \frac{S_{i1}}{E} \tag{13}$$

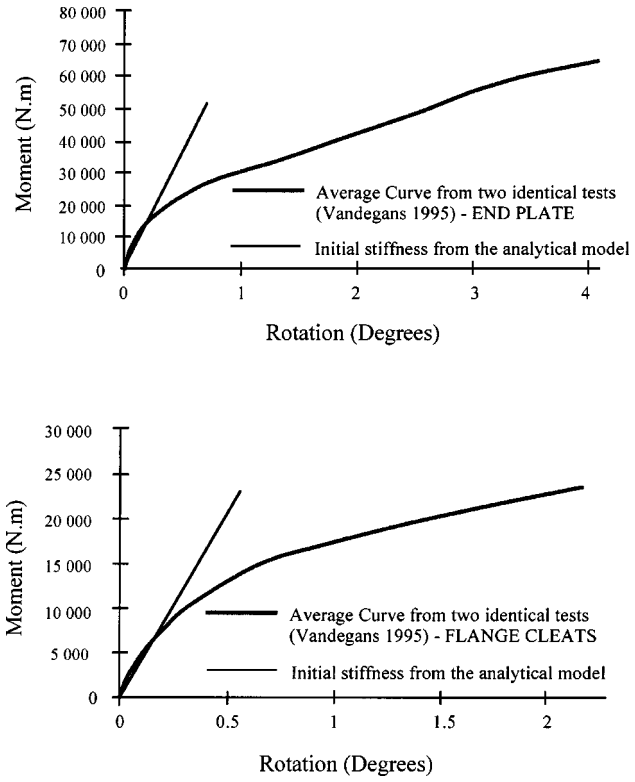

Fig. 11. Comparison of test results from Vandegans (1995) and proposed analytical model for initial stiffness

In Eq. (12) h=the lever arm, defined in Eurocode 3 (1992) as the distance between the center of rotation (in the compression zone) and the center of the upper (tension) area. An illustration is made in Fig. 4 for a flange cleat connection. For other types of connections shown in Fig. 1, h may be taken as: For welded connections h is the distance from the midthickness of the beam tension flange to the midthickness of the beam compression flange (center of compression). For bolted connections with end plates, h is the distance from the center of compression (in line with the midthickness of the beam compression flange) to the bolt row in tension. If there are two or more bolt rows in tension, that distance may be taken as the distance from the center of compression to a point midway between the farthest two bolt rows in tension.

Application of the model requires the evaluation of the various stiffness coefficients, and the evaluation of Eq. (12) for each test result. Fig. 11 illustrates the application of Eq. (12) to the selected experimental tests, showing the initial stiffness calculated using the model proposed in this paper and the experimental results, good agreement being easily observed.

Concluding Remarks

The model described in this paper was able to adequately reproduce the initial rotational stiffness of concrete-filled RHS/I-beam joints. Additionally, the proposed expressions for evaluation of the postlimit stiffness of the component column web/loaded chord in bending, coupled with recently developed closed-form analytical procedures (Silva and Coelho 2001) for the evaluation of the nonlinear moment-rotation response of steel joints in the context of the component method, should enable the solution to an otherwise untreatable problem.

Next, extension to the more complex problem of unfilled RHS/I-beam joints loaded in bending still presents a few shortcomings to be solved: (1) position of center of compression for the various connection types and, consequently, the appropriate lever arm; and (2) influence of the deformation of the side chords. Finally, the influence of the tridimensional behavior of joints (major and minor axis) should also be taken into consideration. These issues are currently being actively addressed.

References

Czechowski, A., Kordjak, J., and Bródka, J. (1987). ''Flexibility formulae and modeling of joint behavior in girders made of rectangular hollow sections.'' *Proc., State-of-the-Art Workshop on Connections and the Behavior, Strength and Design of Steel Structures*, ENS, Cachan, France, Elsevier Applied Science, London, 175–182.

Eurocode 3. (1992). ''Design of steel structures. Part 1.1: General rules and rules for buildings.'' *European Prestandard ENV 1993-1-1*, Commission of the European Communities, Brussels.

FINELG non-linear finite element analysis program; user's manual; release 5. (1990). Univ. of Liège, Belgium.

Gomes, F. C. T. (1996). ''Moment capacity of beam-to-column minor-axis joints.'' *Proc., IABSE Int. Colloquium on Semi-Rigid Structural Connections*, Istanbul, Turkey, IABSE, 319–326.

Gomes, F. C. T., Jaspart, J. P., and Maquoi, R. (1994). ''Behavior of minor axis joints and 3-D joints.'' *Proc., 2nd State-of-the-Art Workshop on Semi-Rigid Behavior of Civil Engineering Structural Connections*, Prague, 111–120.

Jaspart, J. P., Maquoi, R., Guisse, S., Lognard, B., and Taquet, F. (1995). ''Sixième Rap. Sem. Recherche COST C1.'' Univ. de Liège, Belgium (in French).

Korol, R., and Mirza, F. (1982). ''Finite element analysis of RHS T-joints.'' *J. Struct. Div., ASCE*, 108(9), 2081–2098.

Lu, L. H., Puthli, R. S., and Wardenier, J. (1993). ''Semi-rigid connections between plates and rectangular hollow section columns.'' *Proc., 5th Int. Symp. on Tubular Connections*, Nottingham, U.K., E&FN Spon, London, 723–731.

Lu, L. H., and Wardenier, J. (1998). ''The ultimate strength of I-beam to RHS column connections.'' *J. Constr. Steel Res.*, 46, 1–3, Paper no. 139.

Lusas finite element system user manual; release 12. (1996). FEA Ltd., Kingston-upon-Thames, U.K.

Massonet, C., and Save, R. (1972). ''Calcul plastique des constructions—Vol II: Structures dépendant de plusieurs paramètres.'' ASBL, Bruxelles, Belgium (in French).

Matsui, C. (1986). ''Strength and deformation capacity of frames composed of wide flange beams and concrete filled square steel tubular columns.'' *Proc., 1986 Pacific Structural Steel Conf.*, Auckland N.Z., New Zealand Heavy Engineering Research Assoc., 169–181.

Morino, S., Kawaguchi, J., Yasuzaki, C., and Kanazawa, S. (1993). ''Behavior of concrete-filled steel tubular three-dimensional subassemblages.'' *Proc., Composite Construction in Steel and Concrete II*, ASCE, New York, 726–741.

Neves, L. F. C. (1996). ''Semi-rigid connections in steel structures. Assessment of stiffness for minor-axis geometries.'' MSc. thesis, Univ. of Coimbra, Coimbra, Portugal (in Portuguese).

Neves, L. F. C., and Gomes, F. C. T. (1996). ''Semi-rigid behavior of beam-to-column minor-axis joints.'' *Proc., IABSE Int. Colloquium on Semi-Rigid Structural Connections*, Istanbul, Turkey, 207–216.

Neves, L. F. C., and Gomes, F. C. T (1999). ''Guidelines for a numerical modelling of beam-to-column minor-axis joints.'' *COST C1 Rep. of W.G. 6—Numerical Simulation*, K. S. Virdi, ed., European Commision, Brussels, 48–60.

Ricles, J. M., Lu, L. W., Graham, W. W., and Vermaas, G. W. (1997). ''Seismic performance of CFT column-WF beam rigid connections.''

Proc., Engineering Foundation Conf. 1996, ASCE, New York, 282–297.
Shakir-Khalil, H. (1992). ''Full-scale tests on composite connections.'' *Proc., Composite Construction in Steel and Concrete II*, ASCE, New York, 539–554.
Silva, L. S., and Coelho, A. (2001). ''A ductility model for steel connections.'' *J. Constr. Steel Res.*, 57, 45–70.
Silva, L. S., Coelho, A., and Neto, E. (2000). ''Equivalent post-buckling models for the flexural behavior of steel connections.'' *Comput. Struct.*, 77, 615–624.
Ting, L. C., Shanmugam, N. E., and Lee, S. L. (1991). ''Box-column to I-beam connections with external stiffeners.'' *J. Constr. Steel Res.*, 18, 209–226.
Vandegans, D. (1995). ''Liaison entre poutres métalliques et colonnes en profils creux remplis de béton, basée sur la technique du goujonnage.'' *MT 193*, CRIF, Bruxelles.
Vandegans, D. (1996). ''Application de la méthode des composantes selon l'Eurocode 3 aux assemblages par goujons filetés dans le cas de profils creux remplis de béton.'' *Constr. Metallique*, (3), 25–37.
Weynand, K., Jaspart, J. P., and Steenhuis, M. (1995). ''The stiffness model of revised annex J of Eurocode 3.'' *Proc., 3rd Int. Workshop on Connections*, Trento, Italy, 441–452.